About the Nature of the Recirculation Zone Behind a Mach Disk in an Underexpanded Jet

P.A. Skovorodko

Institute of Thermophysics SB RAS, 630090, Novosibirsk, Russia

Abstract. The paper is devoted to the nature of the recirculation zone behind a Mach disk in an underexpanded jet predicted by CFD at some range of determining parameters. The free jet flow behind the axisymmetric sonic nozzle was simulated by two approaches – in the frames of the full set of Navier-Stokes (NS) equations and by the DSMC approach. No recirculation zone predicted by NS algorithm was observed in the flow field obtained by the DSMC approach. The nature of the discussed effect, therefore, seems to be purely computational and caused by limited applicability of the Navier-Stokes equations for the description of the flow in the vicinity of the Mach disk with the high gradients of the flow parameters at that location.

Keywords: Underexpanded free jet, Mach disk, recirculation zone, Navier-Stokes equations, DSMC.
PACS: 02.70.Uu, 05.10.Ln, 47.10.ad, 47.11.Bc, 47.15.Uv, 47.20.-k, 47.32.C-, 47.40.-x, 47.40.Ki, 47.45-n.

INTRODUCTION

In some papers devoted to CFD study of the flow in an underexpanded free jet, the effect of the formation of the recirculation zone behind a Mach disk was discovered [1-6]. This zone represents a toroidal vortex in the near axis region with negative axial velocity. Until now the effect has not had any experimental confirmation. As it is noted in [5] "…at the present state of research it cannot be excluded that the vortex might be of computational origin as a consequence of the (r, z) problem formulation, where screwlike three-dimensional flows are not possible." There is another possibility for the computational nature of the discussed effect – limited applicability of the Navier-Stokes equations for the description of the flow in the vicinity of the Mach disk with the high gradients of the flow parameters at that location.

To clarify the situation, the axisymmetric flow in an underexpanded jet behind the sonic nozzle was simulated by two approaches, namely, in the frames of the full set of unsteady Navier-Stokes equations, that were solved numerically by an original algorithm based on a staggered grid (NS algorithm) [7], and in the frame of the standard DSMC algorithm [8].

PROBLEM FORMULATION

The axisymmetric domain of the simulation for the flow field in an underexpanded free jet is schematically shown in Fig. 1. It includes permeable boundaries 1, 3, 4, solid boundary 2 and the flow centerline 5. Through surface 1, representing the nozzle exit, the gas inflow into the domain takes place. The boundary conditions on surfaces 1-5 were set in accordance with the approach applied for the simulation of the flow field.

NS Algorithm

The NS algorithm representing the numerical method for the solution of unsteady Navier-Stokes equations for compressible perfect gas based on the staggered grid is now well tested and approved. It allows one to simulate a wide variety of problems of sub-, trans- and supersonic gas dynamics [6, 7, 9].

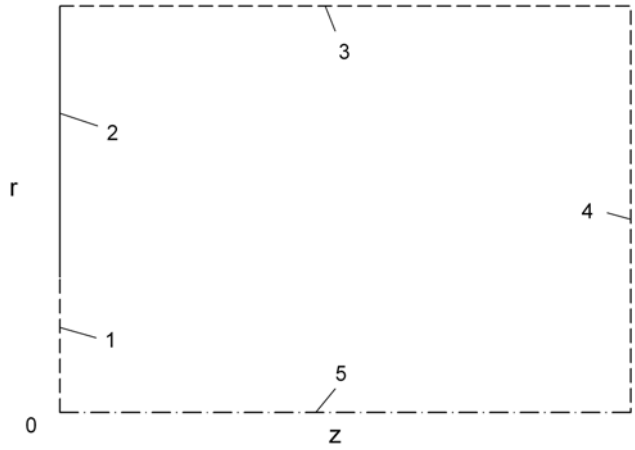

FIGURE 1. The domain of simulation the flow field in underexpanded free jet.

For the NS algorithm the set of determining parameters was as follows: the specific heats ratio $\kappa = 1.4$, the pressure ratio $p_0 / p_\infty = 400$, the temperature ratio $T_0 / T_\infty = 1$, the Reynolds number $\mathrm{Re} = \rho_0 c_0 r_e / \mu_0 = 1500$, the Prandtl number Pr = 0.71, the temperature dependence of viscosity $\mu \sim \sqrt{T}$, the bulk viscosity $\mu' = 0$. The domain of the simulation shown in Fig. 1 was rectangular in shape with dimensions of $30\,r_e$ and $60\,r_e$ in radial and axial directions, respectively. A uniform grid with mesh sizes $dr = dz = 0.1 r_e$ was used. Here indexes $_0$, $_\infty$ and $_e$ are used to denote the variables in stagnation chamber, in the background gas, and on the nozzle exit, respectively, and c is the sound speed.

The considered free jet was assumed to be sonic with a uniform distribution of parameters on surface 1. The temperature of solid surface 2 was assumed to be the same as stagnation temperature ($T_w = T_0$). At this surface the normal component of total velocity (w) was prescribed to be equal to zero while the tangential component (u) as well as the temperature T were defined by taking into account the velocity slip and temperature jump [10] with unit accommodation coefficients. In the developed NS algorithm there is no need to prescribe the pressure or the density at the solid boundaries.

The conditions at the outlet boundaries (3, 4) were defined in the same manner. The axial and radial velocities were obtained by extrapolation from internal points of the domain. The same extrapolation was applied to the density and temperature for the outlet fluxes on these boundaries. For the inlet fluxes the density and temperature were defined assuming the total enthalpy and total pressure to be the same as in the flooded space. At the flow centerline the radial velocity as well as the radial derivatives of the axial velocity and temperature were prescribed to be zero.

DSMC Approach

The simulation of the flow with the same set of determining parameters by the DSMC approach [8] was performed on the same grid used in the NS algorithm with about $2.5 \cdot 10^6$ simulated molecules in the domain of simulation at the steady state. The simulation was performed without the use of radial weighting factors. All the collisions between the molecules were assumed to be inelastic.

As it is known, the boundary conditions for the DSMC approach consist of prescribing the distribution function for only the molecules entering the domain [8]. Therefore, for surface 1 (see Fig. 1) this procedure is straightforward. On solid surface 2 the full accommodation of translational and internal degrees of freedom of incident molecules to the equilibrium values corresponding to the surface temperature was assumed. The setting of boundary conditions on permeable boundaries in the DSMC approach is not a trivial problem. On surface 3 the equilibrium distribution function typical of background gas was assumed – this assumption seems to be quite appropriate for the considered flow since the expected velocities of the gas on this surface are small compared to the sound speed. The same condition applied to surface 4 results in the appearance of strong disturbances of the flow

parameters in the vicinity of this surface due to sufficiently high velocities of the gas here. Two ways to overcome this problem were tested.

One of them (BC1) consists of enlarging the axial size of the domain to a length providing an independence of the flow parameters at the desirable region of the flow from the conditions on surface 4. Test calculation shows that extending the axial size of the domain to the value of $80\,r_e$ is quite sufficient – the axial size or the region of mentioned disturbances was found to be $\leq 20\,r_e$.

Another way (BC2) consists of utilizing at surface 4, placed at the distance $z = 60\,r_e$, the radial profiles of parameters obtained by NS algorithm. Both of these ways predicted similar distribution of flow field parameters inside the region $z \leq 60\,r_e$.

RESULTS AND DISCUSSION

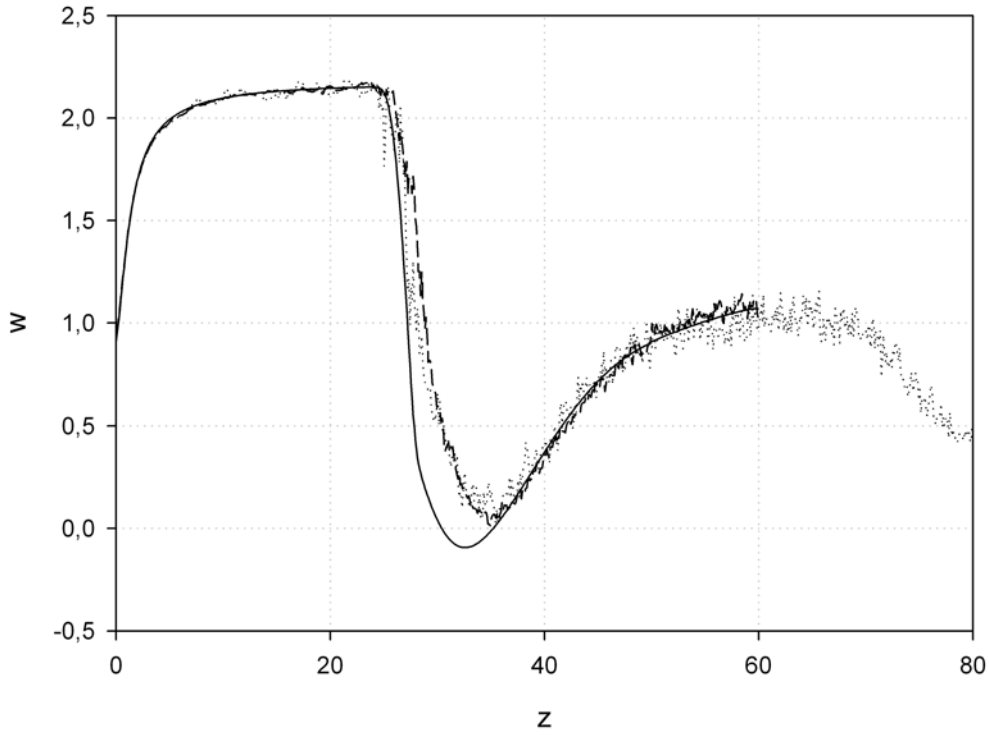

FIGURE 2. The distributions of axial velocity along the centerline (solid line – NS algorithm, dotted line – DSMC approach (BC1), dashed line –DSMC approach (BC2).

Figure 2 illustrates the distributions of axial velocity normalized by c_0 along the centerline (here and below the coordinates r, z are normalized by the radius of nozzle exit r_e). The profiles obtained by the NS algorithm as well as by the DSMC approach with two variants of setting the boundary conditions on surface 4 are shown. As was indicated above, both profiles obtained by the DSMC approach are in good agreement with each other inside the region $z \leq 60$. The significant drop of velocity at $z > 60$ reveals the above mentioned disturbances of the flow field caused by the boundary conditions of type BC1 in the vicinity of surface 4. The boundary conditions of type BC2 seem to give quite reasonable results. In the jet core ($z < 25$) the NS and DSMC data are in good agreement with each other.

As it is seen from Fig. 2, in the entire region the axial velocity obtained by the DSMC approach is positive in contrast with the profile predicted by the NS algorithm with negative velocity for $30.4 < z < 35.2$.

The existence of a region with negative axial velocity indicates the formation of a recirculation zone in the flow field that may be seen from Fig. 3 where the streamlines picture for NS and DSMC (BC2) distributions of parameters are shown. In the NS picture (Fig. 3a) the recirculation zone is well expressed, with its radius about half of the radius of the Mach disk. The DSMC streamline picture (Fig. 3b) is in good agreement with those obtained by

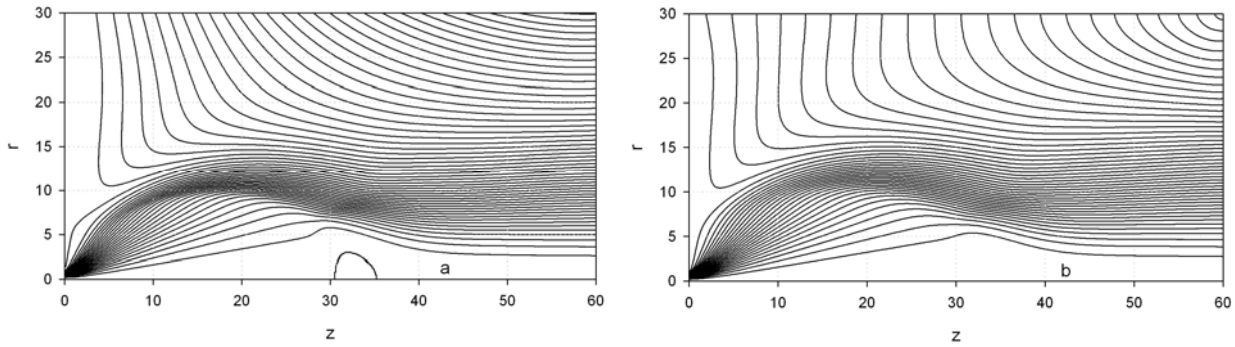

FIGURE 3. The streamline pictures in an underexpanded jet behind the sonic nozzle predicted by NS (a) and DSMC (b) algorithms.

the NS algorithm in almost all the domain except the region behind the Mach disk where no recirculation zone is formed.

Figure 4 illustrates the field of density contours obtained by NS (Fig. 4a) and DSMC (Fig. 4b) algorithms. The pictures reveal the structure typical of an underexpanded free jet with the formation of a Mach disk, barrel shock and triple point. Both pictures are in agreement with each other though in the DSMC field the influence of boundary condition type BC2 is visible in the near vicinity of surface 4 (see Fig. 1) as well as in the right upper corner of the domain. Of course, these small disturbances have negligible effect on the main jet structure. The DSMC approach predicts noticeably larger widths of the Mach disk and of the shock layer between the barrel shock and the jet boundary compared to those obtained by the NS algorithm.

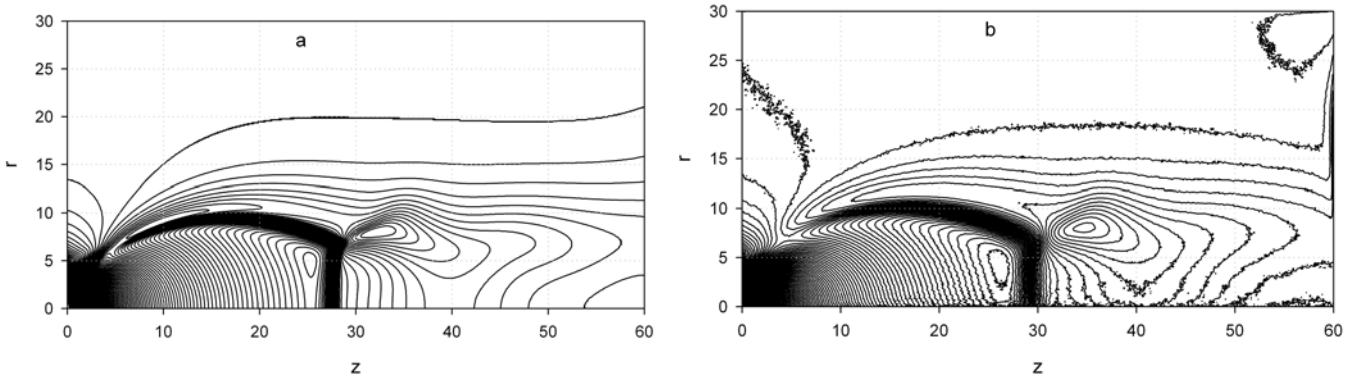

FIGURE 4. The field of density contours in an underexpanded jet behind the sonic nozzle predicted by NS (a) and DSMC (b) algorithms.

To understand the reasons of the fundamental difference of the flow fields obtained by the NS and DSMC approaches (see Fig. 3) let us analyze the applicability of Navier-Stokes equations for the description of the studied flow. It is well known that the Navier-Stokes equations cannot adequately describe the gas flow in a region several mean free paths thick near the surface (the Knudsen layer) as well as in front of a strong shock wave [8]. The latter fluid-dynamic element is present in the flow being considered. We searched for the regions of the flow where the applicability of the continuum approach is questionable by applying the procedure proposed in [11], based on the gradient-length local (GLL) Knudsen number:

$$(Kn)_{GLL} = \frac{l}{Q}\left|\frac{dQ}{ds}\right| \qquad (1)$$

where l is the local mean free path, Q is the flow property (density or temperature), and s is some distance between two points in the flow field. The applicability condition is [11]

$$(Kn)_{GLL-D} < 0.05 \qquad (2)$$

where $(Kn)_{GLL-D}$ is the Knudsen number based on the density ($Q \equiv \rho$). The estimation of the Knudsen number $(Kn)_{GLL-D}$ was made by the relation

$$(Kn)_{GLL-D} = \frac{l}{\rho}\sqrt{\left(\frac{\Delta\rho}{\Delta r}\right)^2 + \left(\frac{\Delta\rho}{\Delta z}\right)^2} \qquad (3)$$

for all the points of the flow field.

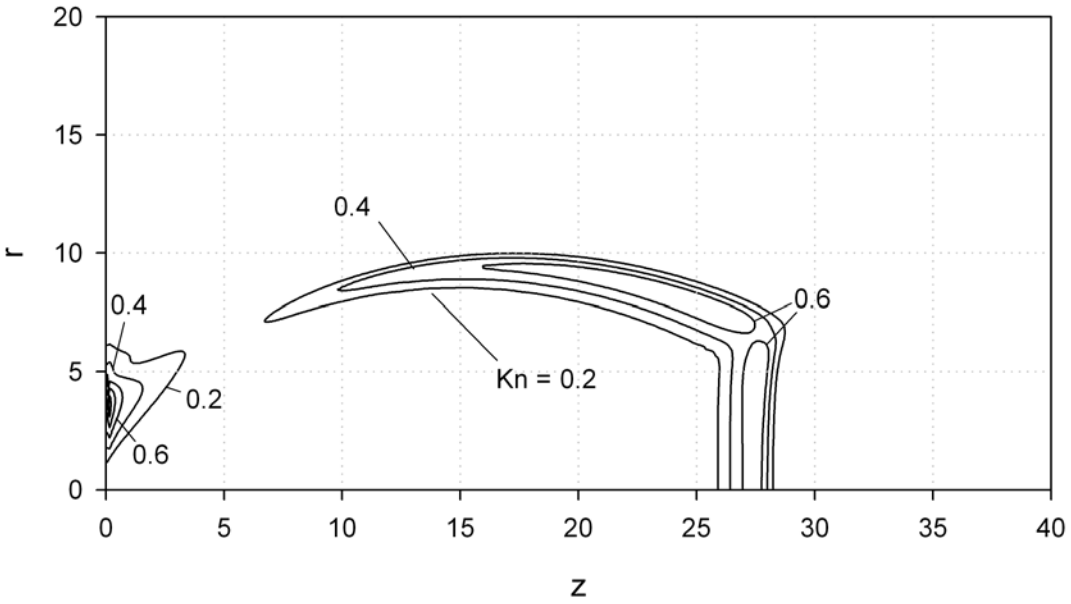

FIGURE 5. The distributions of gradient-length local Knudsen number ($(Kn)_{GLL-D}$) in the flow field obtained by NS algorithm.

Fig. 5 illustrates the distribution of gradient-length local Knudsen number ($(Kn)_{GLL-D}$) in the flow field obtained by the NS algorithm. The lines corresponding to the values of the Knudsen number 0.2, 0.4 and 0.6 are shown. All these lines correspond to the conditions in the flow field where the applicability of Navier-Stokes equation to the description of the flow is questionable (see condition (2)). The shown lines correlate well with the field of density contours plotted in Fig. 4a. In the region far from the nozzle lip the Knudsen number achieves its maximum value ($(Kn)_{GLL-D}$ = 0.77) at the point with coordinates z = 25.65, r = 7.65, i. e. in the vicinity of the triple point (see Fig. 4a). In the vicinity of the nozzle lip the maximum value of the Knudsen number is even higher ($(Kn)_{GLL-D}$ = 1.2), at coordinates z = 0.15, r = 3.55.

CONCLUSION

The main results of the performed study may be summarized as follows:

1. The flow in an underexpanded jet of molecular gas behind the axisymmetric sonic nozzle was simulated by two approaches – in the frames of full set of unsteady Navier-Stokes equations and by the standard DSMC approach.
2. The method of using the Navier-Stokes's profiles of parameters on permeable boundaries as the boundary conditions for the DSMC approach was tested and found to be appropriate.

3. For the studied regime of an underexpanded jet the Navier-Stokes equations predict the formation of recirculation zone behind the Mach disk. Similar features of the flow field have been reported previously in the literature.
4. A DSMC approach to the flow with the same set of determining parameters predicts no formation of a recirculation zone in the flow field.
5. An analysis of the applicability of the Navier-Stokes equations to the description of the considered flow made on the basis of gradient-length local Knudsen number reveals the regions where this applicability is questionable: the vicinity of the nozzle lip, the vicinity of the Mach disk including the triple point, and the shock layer between the barrel shock and the jet boundary.
6. The nature of the discussed effect, therefore, seems to be purely computational and caused by limited applicability of the Navier-Stokes equations for the description of the flow in the vicinity of the Mach disk with high gradients of the flow parameters which are present.

ACKNOWLEDGMENTS

This study was supported by Federal Targeted Program "Research and Educational Staff in Innovation Russia" (contract no. 02.740.11.0109).

REFERENCES

1. C. L. Chen, S. R. Chakravarthy and C. M. Hung, *AIAA J*. **32**, 1836-1843 (1994).
2. T. Stenholm, and V. Jover, "Flow separation control activities at Volvo and SEP," in *ESA Advanced Nozzle Workshop*, University of Rome, Italy, October 1997.
3. B. J. Gribben, F. Cantarini, K. J. Badcock and B. Richards, "Numerical Study of an Underexpanded Jet," in *Proc. Third Eur. Symp. on Aerothermodynamics for Space Vehicles*, ESTEC, ESA SP-426, pp. 111-118 (1998).
4. M. Frey and G. Hagemann, *AIAA Paper* **3619** (1998).
5. B. Mate, I. A. Graur, T. Elizarova, I. Chirokov, G. Tejeda, J. M. Fernandez and S. Montero, *J. Fluid Mech*. **426**, 177-197 (2001).
6. P.A. Skovorodko, *Matematicheskoye modelirovaniye* **15**, 6, 95-100 (2003) (in Russian).
7. A. Broc, S. De Benedictis, G. Dilecce, M. Vigliotti, R. G. Sharafutdinov and P. A. Skovorodko, *J. Fluid Mech*. **500**, 211-237 (2004).
8. G.A. Bird, *Molecular Gas Dynamics and the Direct Simulation of Gas Flows*, Oxford, Clarendon Press, 1994.
9. J.C. Lengrand, V.G. Prikhodko, P.A. Skovorodko, I.V. Yarygin and V.N. Yarygin, "Outflow of Gas from Nozzle with Screen into Vacuum," in *Rarefied Gas Dynamics: 26th International Symposium*, edited by T. Abe, AIP Conference Proceedings 1084, American Institute of Physics, Melville, NY, 2009, pp. 1158-1163.
10. Rae, W. J. *AIAA J*. **5**, 811–820 (1971).
11. I. D. Boyd, G. Chen and G. V. Candler, *Phys. Fluids*, **7**, 210–219 (1995).